Macromolecular Chemistry and Physics
www.mcp-journal.de

# Investigation of the Porosity of Poly(sodium methacrylate) Hydrogels by $^1$H-NMR $T_2$-Relaxation and Inverse Size-Exclusion Chromatography

*Christoph Pfeifer, Federica Cavalli, Birgit Huber, Patrick Theato,* Leonie Barner,* and Manfred Wilhelm**

**AbstractA series of poly(sodium methacrylate) hydrogels, also called superabsorbents, having a theoretical degree of neutralization of 100 mol%, and degree of crosslinking varying from 0.6 to 20 mol%, are synthesized via conventional free radical polymerization. The networks are characterized in detail by inverse size-exclusion chromatography and $^1$H-NMR relaxometry in order to place particular emphasis on the investigation of the pore size distribution (PSD) and the chain mobility, respectively. The two previously mentioned parameters are compared to understand the correlation between the elastic chain mobilities and the average pore size of the hydrogel. From the resulting data, a new empirical equation is proposed, which is valid under the given experimental conditions and permits a rough estimation of the average PSD from the relaxation data. Thus, the equation permits to reduce the number of analytical techniques needed for the characterization of complex systems such as polymer networks.**

## 1. Introduction

Superabsorbent polymers (SAPs) are a class of materials used in numerous applications[1] that include diapers,[2] underwater cable insulations,[3] and water-releasing agents for agriculture in dry regions.[4] The driving force behind the use of SAPs is their ability to absorb large amounts of water, up to 1000 times their own weight in the dry state.[5,6] The high affinity for water arises from the presence of hydrophilic groups,[7] and is substantially enhanced by the presence of charges along the polymer backbone.[8,9] At the same time, the crosslinking points connect polymer chains to each other, preventing the dissolution.[10]

The crosslinking points and the elastic chains form the microstructure of the network.[11] In a simplified scenario, the network microstructure can be imagined as a net, where the combination of polymer chains and junction points results in voids, called pores.[11,12] It becomes clear that the size of these pores decreases with increasing amount of crosslinking agent, as the amount of crosslinking points increases.[13]

In reality, the porosity of hydrogels is also influenced by random events occurring during the synthesis.[12,14] The aforementioned random events generate particular localized topologies, such as closed loops and entanglements, which modify the microstructure and therefore affect the porosity of the final hydrogel.[12,15] For this reason, loops and entanglements are often referred to as "defects."[11] The formation of such defects is inevitable but it is more likely when the hydrogels are synthesized via conventional free radical polymerization (FRP) of a monovinyl or divinyl monomer.[12,14,16–20] Despite this fact, FRP methods are widely utilized in industry due to the simplicity of their setup, the fast reaction times, and the wide variety of monomers that can be used.[21] In return, a lower control over the network architecture and a larger pore size distribution (PSD) is obtained, which particularly affects the swelling ability.[22,23] Consequently, materials scientists and synthetic chemists intend to determine the porosity of materials to tailor design hydrogels, and maximize the performances according to the desired application.[24]

C. Pfeifer, Dr. F. Cavalli, Prof. P. Theato, Prof. M. Wilhelm
Institute for Chemical Technology and Polymer Chemistry
Karlsruhe Institute of Technology
Engesserstrasse 18, Karlsruhe 76131, Germany
E-mail: patrick.theato@kit.edu; manfred.wilhelm@kit.edu

B. Huber, Prof. P. Theato
Soft Matter Synthesis Laboratory
Institute for Biological Interfaces III (IBG3)
Karlsruhe Institute of Technology (KIT)
Hermann-von-Helmholtz-Platz 1, Eggenstein-Leopoldshafen 76344, Germany

Prof. L. Barner
Centre for Materials Science
School of Chemistry and Physics
Institute for Future Environments
Queensland University of Technology
2 George St, Brisbane, QLD 4000, Australia
E-mail: leonie.barner@qut.edu.au

The ORCID identification number(s) for the author(s) of this article can be found under https://doi.org/10.1002/macp.202000300.



**DOI: 10.1002/macp.202000300**

The porosity of rigid materials, such as silica particles,[25] zeolites,[26,27] or metal–organic frameworks, is commonly determined via Brunauer–Emmett–Teller analysis,[28,29] where the amount of nitrogen adsorbed within the pores is taken into consideration.[30] Mercury intrusion porosity is another adsorption-based technique for the estimation of the porosity of materials.[31,32] However, these methods have the disadvantage that they are limited to polymer porosity in the dry state. Consequently, the measured porosity does not reflect the void structure of the networks in the swollen state of the hydrogel, which is the one used during the application.[33] In literature, different methods have been proposed for the scope of network characterization that involve in most cases the diffusion of species with a well-defined size within the network.[34,35] These species can be either magnetic particles or non-charged polymers. The former require the use of a magnetic field for the detection, while the latter simply use a chromatographic technique known as inverse size-exclusion chromatography (iSEC).[36]

Contrary to conventional SEC, the main concept of iSEC is based on characterizing a network material with defined samples rather than soluble polymer samples of unknown size eluting from a defined porous column material.[36–38] With the absolute retention time being dependent on the porosity of the matrix, a series of polymer standards with well-defined molecular weights and hydrodynamic radii, dissolved in the eluent used as the mobile phase and the hydrogel itself used as the porous matrix, one can invert the concept of SEC and determine the porosity of the column material, which is in our case the hydrogel itself.[33,37,39] The advantage of iSEC is to access data on porosity with a relative simple setup, yet without challenging the SEC column filling and measurement procedures. Herein, not only an optimized procedure for poly(sodium methacrylate) (PSMA) hydrogels is proposed but also the comparison between two different analytical techniques is presented. Moreover, iSEC is compared to $^{1}$H-NMR relaxometry, which probes the mobility of the elastic chains and the PSD of the microstructure, respectively. The difference in chain mobility is in fact attributed to a different chain lengths and thus to an inhomogeneity in the pore sizes within the hydrogel. Thus, the goal is to provide a practical equation to correlate these two data sets and enlarge the amount of information obtainable from a single analysis, i.e., $^{1}$H-NMR relaxometry.[40,41]

The present study is performed on a series of PSMA hydrogels, having a degree of neutralization (DN) of 100 mol% and a degree of crosslinking (DC) varying from 0.3 to 20 mol% to cover a wide range from soft to highly crosslinked hydrogels. At first, the hydrogels were synthesized via conventional FRP, which was chosen to apply the study to one of the most commonly used polymer networks. Thereafter, samples were tested for their water absorbency, simply by performing swelling experiments, while the local mobility was investigated upon performing $^{1}$H-NMR relaxometry measurements. Lastly, iSEC measurements were conducted and optimized for the investigation of the PSD.

## 2. Results and Discussion

The synthesis and the removal of the unreacted fractions from the network were performed by extraction with distilled water according to the procedure described in the Supporting Information. Afterwards, swelling experiments were performed by exposing the networks to a large excess of aqueous 1 wt% NaCl solution overnight. The use of NaCl solution mimics their use in application an also leads to a defined charge density, respective Debye length. The procedure is detailed in the Supporting Information and the results are plotted in **Figure 1**.

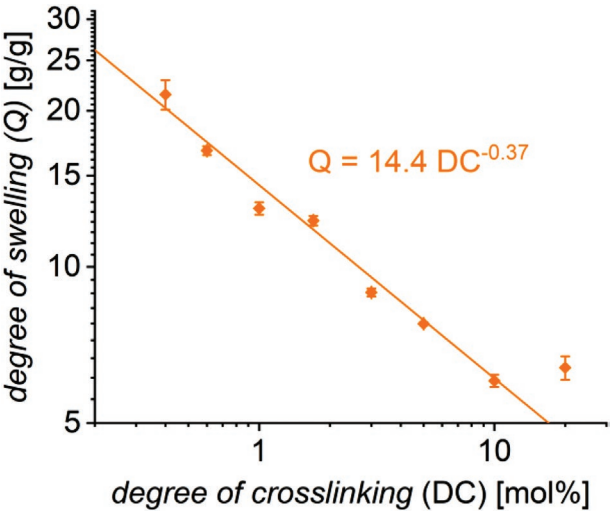


**Figure 1.** Degree of swelling at equilibrium $Q$, expressed as mass ratio ($g_{H_2O}/g_{polymer}$) as a function of crosslinking DC for a series of poly(methacylic acid) networks synthesized via conventional FRP and having a degree of neutralization of 100 mol%. The results represent the ability of networks to swell in an aqueous solution of 10 g mol$^{-1}$ NaCl.

Figure 1 shows that the water uptake diminishes with increasing DC. More precisely, this relation can be described by a power law dependency and the results are in agreement with the Flory–Rehner theory, which first described the behavior of polymer networks in contact with a solvent. The water uptake is a compromise between the natural tendency of hydrophilic groups to interact with water molecules, which on the one hand cause the stretching of the chains, and the physical constraint caused by the crosslinking points, which on the other hand keep the chains linked together and hence prevents swelling beyond a certain degree. Despite the importance of knowing the swelling ability of a material in the context of its further applications, this analysis does not provide any precise information on the microstructure or on the pore size of the hydrogel.

Thus, with the aim of gaining more insight into the polymer architecture, the hydrogel samples were analyzed via $^{1}$H-NMR relaxometry. The decay resulting from the $T_2$-relaxation of the net magnetization can be linked to the mobility of chain segments via their autocorrelation function. The crosslinking points in the network bring further constrains into the system enabling first assumptions on structural heterogeneity.[40,42] The experiments were recorded following a slightly optimized procedure compared to the one reported in the literature,[41,43] and the adopted pulse sequences are carefully described in the Supporting Information together with a detailed description of the theoretical background of the method.

The deconvolution of the raw data was conducted using the Contin approach, which was implemented into a MATLAB

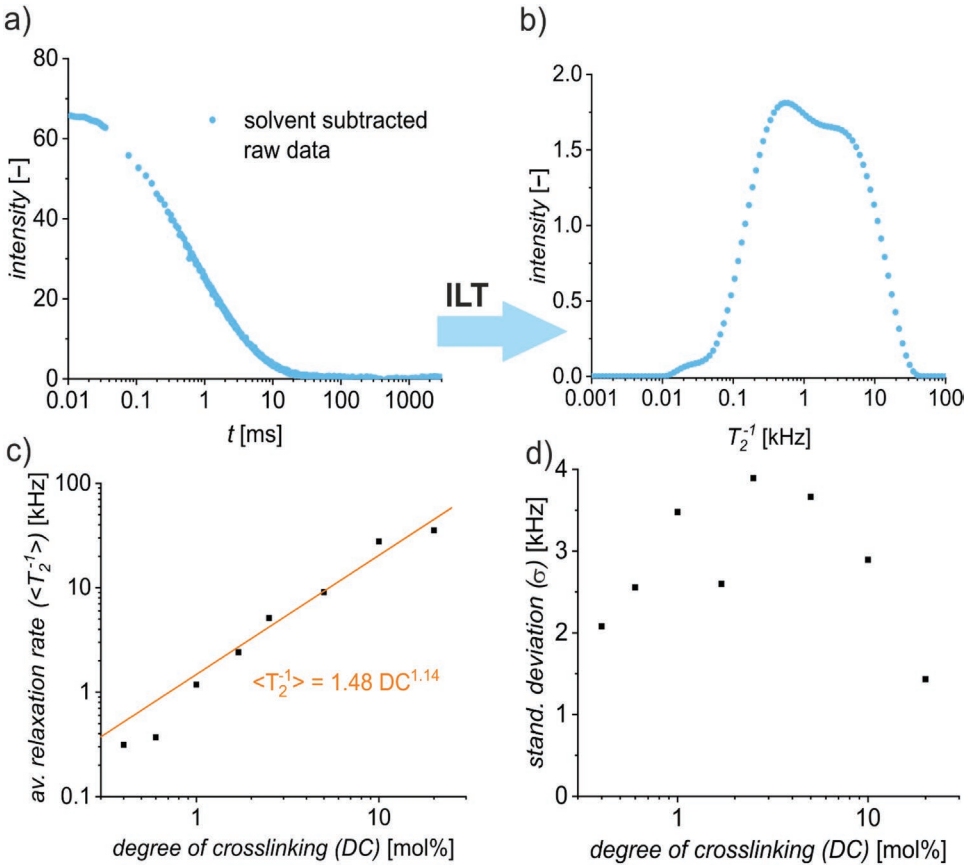


**Figure 2.** a) $T_2$-relaxation curve and b) deconvoluted decay using the inverse Laplace transformation (ILT, 100 data points, $\alpha = 10$) for poly(methacrylic acid) hydrogel synthesized via conventional FRP fixing a degree of neutralization of 100 mol% and DC = 1 mol%. c) Average mobility and d) standard deviation for several poly(methacrylic acid) hydrogels synthesized via conventional FRP fixing a degree of neutralization of 100 mol% and with a DC that varies from 0.6 to 20 mol%.

script by Ryland et al.[44,45] Here, the present relaxation rates are extracted by an inverse Laplace transformation as thoroughly explained in the Supporting Information. For the sake of clarity, in the main text, only one sample will be presented in detail, while the results for the other samples can be found in the Supporting Information. Thus, herein the raw and elaborated data for PSMA-DC1 are depicted in **Figure 2**a,b, respectively.

In Figure 2 it is noticeable that the networks are best represented by a distribution of relaxation rates (i.e., mobilities) rather than a single mobility. This behavior is in agreement with previous studies and is justified by the complexity of the microstructure of networks.[46] The microstructure is in fact composed of elements having both higher mobility (e.g., free dangling polymer chains) and lower mobility (e.g., close to junction points). Moreover, the formation of dangling ends and entanglements during the synthesis increases the amount of mobile and rigid fractions, respectively. Therefore, since the analyzed network was synthesized via FRP, a broad distribution is expected.

The distribution of relaxation rates is characterized by its average and the related standard deviation σ. The average relaxation rate $< T_2^{-1} >$ could be reasonably associated to the average mobility of the chains itself,[40,47] and thus, could be a characteristic parameter for representing the local mobility within the network. Consequently, by changing the DC, also the average chain mobility should change, as the lengths of the chains are modified. To verify the validity of the latter statement, each network was analyzed via $^1$H-NMR relaxometry. The raw and the deconvoluted data can be found in Figure 2a,b, while the average chain mobility is plotted against the DC in Figure 2c. As anticipated, Figure 2c shows how the chain mobility is reduced if the DC increases. In detail, the average relaxation rate increases from 0.030 to 35 kHz when the DC increases from 0.6 to 20 mol%.

In the next step, the PSD was investigated via inverse SEC (iSEC). As previously mentioned, iSEC offers the possibility to investigate the PSD in a cost-efficient and simple way, without destroying the material during the analysis. Here, the hydrogel was allowed to swell overnight (≈16 h) before the measurement. After swelling, the hydrogel was placed within a glass column with adjustable pistons, and densely packed until no gaps were visible. A detailed description of the adopted procedure is provided in the Supporting Information. Subsequently, a series of pullulan-based polymeric standards were passed through the column in a phosphate-buffered solution. For a complete characterization of each sample, at least 13 different standards were used with a molecular weight range of 180–708.000 g mol$^{-1}$. For a given hydrogel, each polymer standard was characterized

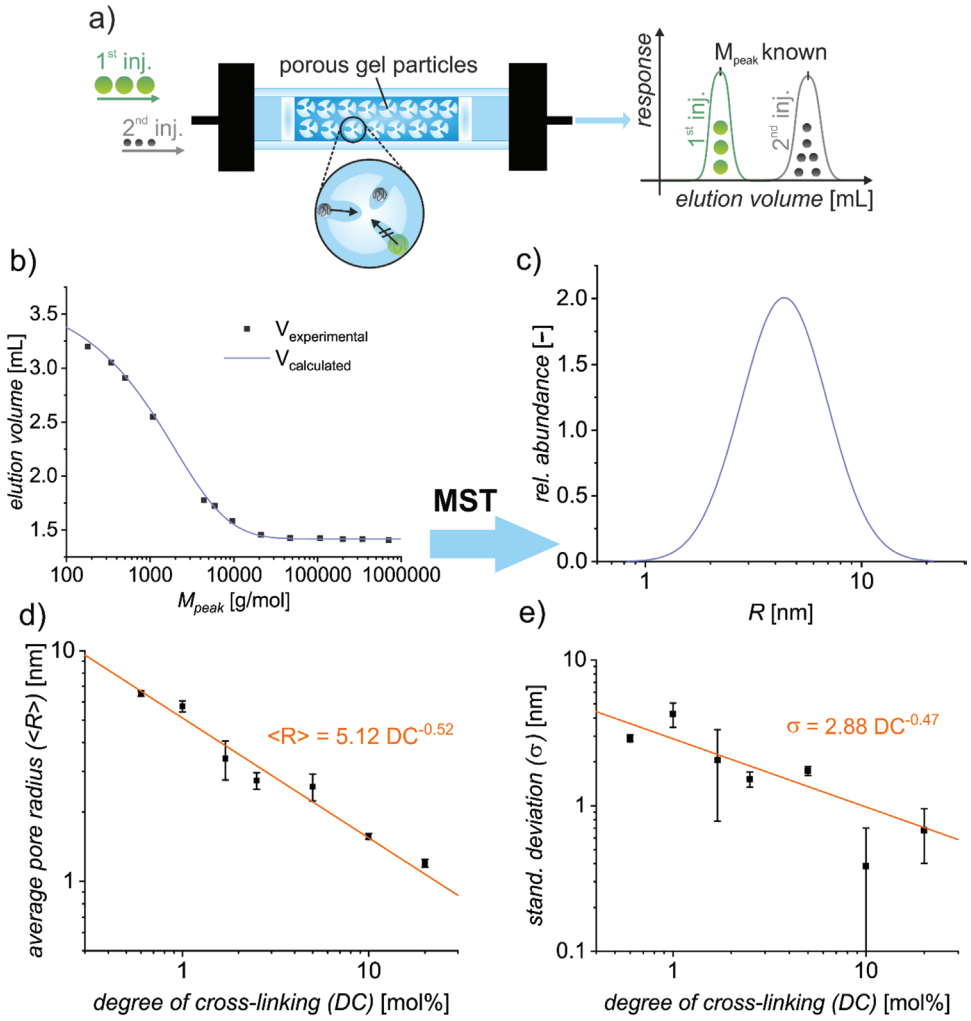


**Figure 3.** a) Schematic representation of the iSEC setup. A series of pullulan standards with known molecular weights were passed through the hydrogel stationary phase. b) Elution volumes of different pullulan standards. c) The elugram was converted by the commercial PoroCheck software V2.5, based on the molecular statistical theory (MST), into the respective pore size distributions. In this case, the sample PSMA-DC5.0-FRP is depicted. d) Average pore radius and e) the standard deviation of the pore size distribution derived from a series of PSMA networks having a DC from 0.6 to 20 mol%.

by its respective retention times, which strictly depends on the ability of the standard to enter as many pores as possible. Comparable to every chromatographic technique, the smaller the hydration radius of the pullulan standards, the higher the ability of pullulan to enter the pores of the hydrogel and the longer the pullulan remains within the hydrogel (high retention time). A visualization of the employed iSEC setup is depicted in **Figure 3**a. Hence, every given pullulan standards will have different retention times in each hydrogel as the porosity changes. Consequently, as the retention time and the molecular weight of the employed pullulan standard are known, the PSD of the stationary phase (i.e., hydrogel) can be calculated. For the sake of clarity, the experimental procedure and the mathematical equations necessary to convert from retention time to the PSD, with the average radius $\langle R \rangle$ and the standard deviation σ, are detailed in the Supporting Information. Exemplarily, the raw data and the final PSD for the hydrogel PSMA-DC5.0 are shown in Figure 3b,c, respectively, while the PSD of the other samples are depicted in the Figure S2, Supporting Information.

In order to have a reliable PSD, the analysis was repeated six times, with repacking of the column for every second measurement. Thereafter, the analysis was performed on the remaining hydrogel samples. As mentioned, the only difference between the hydrogel samples was the DC, which is one of the main parameters influencing the pore size. To visualize that, the average radius ($\langle R \rangle$) of the PSD and its standard deviation are plotted against the DC as shown in Figure 3d,e, respectively.

The wide range of molecular weights of the Pullulan samples were necessary to cover the pore size range present in each of the different hydrogel stationary phases, as displayed in Figure 3b. The peak shown in Figure 3c represents the PSD obtained based on the retention times of Figure 3b. Moreover, by inspecting Figure 3d, one can notice that the average pore radius diminishes with increasing DC. The value decreases from 6.5 to 1.2 nm for networks having a DN = 100 mol% and a DC from 0.6 to 20 mol%, respectively. The decrease of the average pore radius is expected as higher crosslinker concentrations lead to shorter average chain lengths between

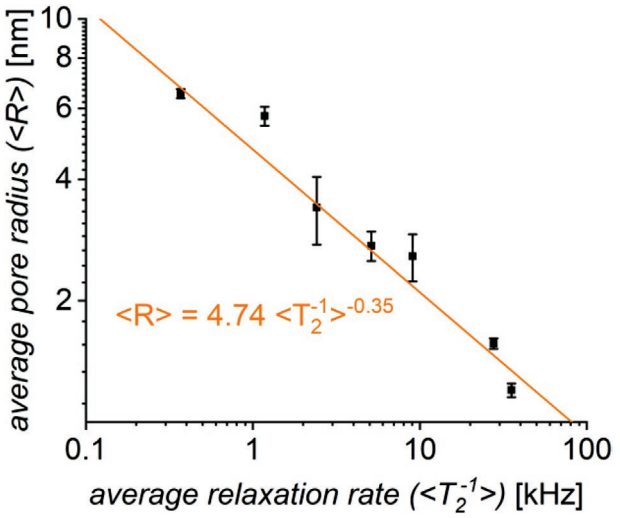


**Figure 4.** Correlation of the average pore radius as obtained by iSEC and the average relaxation rate (i.e., chain mobility) as derived from $^1$H-NMR relaxometry.

the crosslinking points, which define the size of the meshes. The validity of the results is further supported by the swelling tests, previously shown in Figure 1. A smaller pore radius in fact lowers the expansion capability of the microstructure and, as a consequence, the ability to absorb water. The extent of the standard deviations of the average pore radius, shown in Figure 3e, indicates a very broad PSD. The latter findings agree with the large distributions of chain mobility reported in Figure 2b, and the main reason lies in the choice of the synthetic method, here being the conventional FRP.

Lastly, the main objective of the current work is to find a correlation between the average $T_2$-relaxation rate and the average pore size. For this purpose, the two data sets are compared in **Figure 4**.

Figure 4 indicates an empirical power dependency between the two sets of data, which can be expressed by Equation (1)

$$<R> = 4.74 <T_2^{-1}>^{-0.35} \quad (1)$$

Clearly, the validity of Equation (1) is limited to the experimental procedure previously described and under the strict condition of a monomodal distribution of the chain mobility and pore-size distribution. However, the availability of Equation (1) allows for an approximate estimation of the average PSD of its polymer network simply by performing $^1$H-NMR relaxometry, which was performed on a commercially available and affordable benchtop NMR spectrometer, without the need of multiple experiments. This value for the PSD under application related conditions, i.e., in solvent, can be of clear advantage for selected utilizations, such as catalysis, size exclusion of molecules, storage devices, and many more.

## 3. Conclusions

In conclusion, the presented study shows a complete characterization on a series of PSMA hydrogel networks synthesized via conventional FRP, which were entirely charged and had a DC of 0.6–20 mol%. The samples were tested first for water absorbency using a NaCl solution (10 g mol$^{-1}$), where the absorbency varied between 6.4 and 28 g g$^{-1}$ following a power law dependency with a scaling exponent of –0.37 when increasing the DC. Subsequently, the $T_2$-relaxation rate, studied via $^1$H-NMR relaxometry, showed a broad chain mobility distribution as an indication of an inhomogeneous network microstructure. The inhomogeneity in the network microstructure is mainly reflected on a broad PSD, as was demonstrated via inverse SEC. Despite the broad PSD, it was possible to identify the average pore size, which decreased from 6.5 to 1.2 nm when varying the crosslinking agent from 0.6 to 20 mol% in the networks. Lastly, the local chain mobility of the network and the relative average pore size have been compared, and an empirical power exponent of –0.35 was found between the two. Even though the current study is limited to hydrogels having a single DC, it offers the reader a simplified tool for understanding the average PSD of the network simply by knowing the average relaxation rate, and enlarges the amount of information accessible with one technique, i.e., $^1$H-NMR relaxometry.

## Supporting Information

Supporting Information is available from the Wiley Online Library or from the author.

## Acknowledgements

C.P. and F.C. contributed equally to this work. The authors acknowledge financial support by the DFG via project C1 of the SFB1176 "Molekulare Strukturierung weicher Materie."

Open access funding enabled and organized by Projekt DEAL.

## Conflict of Interest

The authors declare no conflict of interest.

## Keywords

hydrogels, inverse size-exclusion chromatography, poly(sodium methacrylate), porosity, $T_2$ relaxation

Received: September 8, 2020
Revised: November 12, 2020
Published online: December 9, 2020

[1] F. L. Buchholz, *J. Chem. Educ.* **1996**, *73*, 512.
[2] F. Masuda, in *Superabsorbent Polymers* (Eds: F. L. Buchholz, N. A. Peppas), American Chemical Society, Washington, DC **1994**, p. 88.
[3] M. J. Zohuriaan-Mehr, H. Omidian, S. Doroudiani, K. Kabiri, *J. Mater. Sci.* **2010**, *45*, 5711.
[4] F. L. Buchholz, A. T. Graham, *Modern Superabsorbent Polymer Technology*, John Wiley & Sons, New York **1998**.
[5] J. Ricka, T. Tanaka, *Macromolecules* **1984**, *17*, 2916.
[6] W. Oppermann, in *Polyelectrolyte Gels* (Eds: R. S. Harland, R. K. Prud), American Chemical Society, Washington, DC **1992**, p. 159.

[7] R. A. Orwoll, P. A. Arnold, in *Physical Properties of Polymers Handbook* (Ed: J. E. Mark), Springer, New York **2007**, p. 233.
[8] H. H. Hooper, J. P. Baker, H. W. Blanch, J. M. Prausnitz, *Macromolecules* **1989**, *23*, 1096.
[9] U. Schröder, W. Oppermann, in *Physical Properties of Polyelectrolyte Gels*, John Wiley & Sons, New York **1996**, p. 19.
[10] P. J. Flory, J. Rehner, *J. Chem. Phys.* **1943**, *11*, 512.
[11] J. E. Mark, *Physical Properties of Polymers Handbook*, Springer, New York **2007**.
[12] J. C. Hernández-Ortiz, E. Vivaldo-Lima, *Handbook of Polymer Synthesis, Characterization, and Processing*, Wiley, Hoboken, NJ **2013**.
[13] P. J. Flory, M. Gordon, P. J. Flory, N. G. McCrum, *Proc. R. Soc. London, Ser. A* **1976**, *351*, 351.
[14] G. Hild, *Prog. Polym. Sci.* **1998**, *23*, 1019.
[15] R. Everaers, K. Kremer, in *Encyclopedia of Materials: Science and Technology* (Eds: K. H. J. Buschow, R. W. Cahn, M. C. Flemings, B. Ilschner, E. J. Kramer, S. Mahajan, P. Veyssière), Elsevier, Oxford **2001**, p. 5724.
[16] G. Beinert, A. Belkebir-Mrani, J. Herz, G. Hild, P. Rempp, *Faraday Discuss. Chem. Soc.* **1974**, *57*, 27.
[17] K. Dušek, M. Dušková-Smrčková, *Prog. Polym. Sci.* **2000**, *25*, 1215.
[18] R. Henkel, P. Vana, *Macromol. Chem. Phys.* **2014**, *215*, 182.
[19] D. M. Kroll, S. G. Croll, *Polymer* **2015**, *79*, 82.
[20] S. Seiffert, *Polym. Chem.* **2017**, *8*, 4472.
[21] P. Nesvadba, *Encyclopedia of Radicals in Chemistry, Biology and Materials*, Wiley, Hoboken, NJ **2012**.
[22] F. Ganji, F. S. Vasheghani, F. E. Vasheghani, *Iran. Polym. J.* **2010**, *19*, 375.
[23] J. H. Ward, N. A. Peppas, *Macromolecules* **2000**, *33*, 5137.
[24] G. Hild, *Polymer* **1997**, *38*, 3279.
[25] I. Ab Rahman, V. Padavettan, *J. Nanomater.* **2012**, *2012*, 132424.
[26] K. Hor, J. Chee, M. N. Chong, B. Jin, C. Saint, P. E. Poh, R. Aryal, *J. Cleaner Prod.* **2016**, *118*, 197.
[27] A. Galarneau, D. Mehlhorn, F. Guenneau, B. Coasne, F. Villemot, D. Minoux, C. Aquino, J.-P. Dath, *Langmuir* **2018**, *34*, 14134.
[28] W. Lu, Z. Wei, D. Yuan, J. Tian, S. Fordham, H.-C. Zhou, *Chem. Mater.* **2014**, *26*, 4589.
[29] Y.-S. Bae, A. Ö. Yazaydın, R. Q. Snurr, *Langmuir* **2010**, *26*, 5475.
[30] S. Brunauer, P. H. Emmett, E. Teller, *J. Am. Chem. Soc.* **1938**, *60*, 309.
[31] G. P. Matthews, A. K. Moss, M. C. Spearing, F. Voland, *Powder Technol.* **1993**, *76*, 95.
[32] J. Urban, S. Eeltink, P. Jandera, P. J. Schoenmakers, *J. Chromatogr. A* **2008**, *1182*, 161.
[33] P. DePhillips, A. M. Lenhoff, *J. Chromatogr. A* **2000**, *883*, 39.
[34] S. Seiffert, *Prog. Polym. Sci.* **2017**, *66*, 1.
[35] M. Hess, E. Roeben, A. Habicht, S. Seiffert, A. M. Schmidt, *Soft Matter* **2019**, *15*, 842.
[36] A. Sepsey, I. Bacskay, A. Felinger, in *Advances in Chromatography* (Eds: N. Grinberg, P. W. Carr), CRC Press, Boca Raton, FL **2017**, p. 205.
[37] Y. Yao, A. M. Lenhoff, *J. Chromatogr. A* **2004**, *1037*, 273.
[38] E. Viktorova, A. Korolev, T. Ibragimov, A. Kurganov, *Polym. Sci., Ser. A* **2011**, *53*, 899.
[39] I. Bacskay, A. Sepsey, A. Felinger, *J. Chromatogr. A* **2014**, *1339*, 110.
[40] K. Saalwächter, J.-U. Sommer, *Macromol. Rapid Commun.* **2007**, *28*, 1455.
[41] J. Höpfner, G. Guthausen, K. Saalwächter, M. Wilhelm, *Macromolecules* **2014**, *47*, 4251.
[42] K. Saalwächter, S. Seiffert, *Soft Matter* **2018**, *14*, 1976.
[43] F. Cavalli, C. Pfeifer, L. Arens, L. Barner, M. Wilhelm, *Macromol. Chem. Phys.* **2019**, *221*, 1900387.
[44] P. Callaghan, S. Godefroy, B. Ryland, *J. Magn. Reson.* **2003**, *162*, 320.
[45] P. Callaghan, S. Godefroy, B. Ryland, *Magn. Reson. Imaging* **2003**, *21*, 243.
[46] X. Guo, C. Pfeifer, M. Wilhelm, B. Luy, G. Guthausen, *Macromol. Chem. Phys.* **2019**, *220*, 1800525.
[47] N. Bloembergen, E. M. Purcell, R. V. Pound, *Phys. Rev.* **1948**, *73*, 679.